Ab initio comparative study of the Cu-In and Cu-Sn intermetallic phases in Cu-In-Sn alloys

S. Ramos de Debiaggi, C. Deluque Toro, G.F. Cabeza, A. Fernández Guillermet

PII: S0925-8388(12)01132-2
DOI: http://dx.doi.org/10.1016/j.jallcom.2012.06.138
Reference: JALCOM 26589

To appear in:

Received Date: 24 April 2012
Revised Date: 15 June 2012
Accepted Date: 30 June 2012

Please cite this article as: S.R. de Debiaggi, C. Deluque Toro, G.F. Cabeza, A. Fernández Guillermet, Ab initio comparative study of the Cu-In and Cu-Sn intermetallic phases in Cu-In-Sn alloys, (2012), doi: http://dx.doi.org/10.1016/j.jallcom.2012.06.138

Ab initio comparative study of the Cu-In and Cu-Sn intermetallic phases in Cu-In-Sn alloys

S. Ramos de Debiaggi [a,b], C. Deluque Toro[a] , G. F. Cabeza [b,c], A. Fernández Guillermet [b,d]

[a] *Facultad de Ingeniería, Universidad Nacional del Comahue, Buenos Aires 1400, (8300) Neuquén, Argentina*

[b] *CONICET*

[c] *Dpto. de Física. Universidad Nacional del Sur, Bahía Blanca. Argentina*

[d] *Centro Atómico Bariloche e Instituto Balseiro, Avda. Bustillo 9500, (8400) Bariloche, Argentina*

The present paper reports a comparative account of the structural, cohesive and thermodynamic stability properties of the binary intermetallic phases (IPs) occurring in the Cu-In and the Cu-Sn phase diagrams, both at low and at high temperatures, based upon systematic density-functional-theory (DFT) calculations. Using the projector augmented wave method and the exchange and correlation functions of Perdew and Wang in the generalized gradient approximation (GGA), as well as the local-density-approximation (LDA) with the Ceperley and Alder exchange and correlation potentials, we determine the lattice-parameters, molar volume, bulk modulus and its pressure derivative, the electronic density of states (DOS) and the energy of formation (EOF) from the elements of the -Cu_7In_3 (aP40), -Cu_9In_4 (cP52) and $CuIn_2$ (tI12) compounds of the Cu-In system. Moreover, DFT-GGA calculations were performed for the compounds: -Cu_4Sn (cF16), -$Cu_{10}Sn_3$ (hP26), -Cu_3Sn both in the (oP8) structure and the (oP80) superstructure, ´-Cu_6Sn_5 (mC44) and -Cu_5Sn_4 both in the $_1$ (mP36) and $_2$ (mC54) structural forms. In addition, the hypothetical structures obtained by replacing In (or Sn) by Sn (or In) are studied, because of their relevance in the CALPHAD modeling of the Cu-In-Sn phase diagram. The work includes a discussion of the composition dependence of the structural and equation-of-state parameters, the electronic DOS, the EOF of the compounds and the differences between the results of the GGA or LDA calculations and the measured values. Besides, various quantities expressing the relative stability of the IPs are introduced and compared with experimental data and with indirect information obtained in a CALPHAD-type two-sublattice modeling of the Cu-In-Sn phase diagram.

Keywords: *ab-initio calculations; transition metal alloys and compounds; Cu-In and Cu-Sn intermetallics; lead-free soldering alloys; thermodynamic properties; thermodynamic modeling*

1. Introduction

The Cu-In-Sn system has been the subject of considerable attention in connection with the use of the In-48 at%Sn eutectic alloy as a soldering material for Cu, which is the usual contact element in electronic and microelectronic applications. This In-Sn alloy is attractive because it has a low liquidus temperature, shows good wettability and the Cu-In-Sn phase diagram indicates that several intermetallic phases (IPs) form with Cu [1]. Because of this interesting combination of properties, several experimental studies of the reactions between Cu and the In-Sn alloys have been reported in the last decades [2,3]. A key finding of the recent work is that the ternary IPs occurring between 473 and 673 K at the interconnection zone in Cu/In-Sn/Cu joints are those formed by incorporating In or Sn to the binary compounds stable in the subsystems Cu-Sn and Cu-In, respectively [3]. In view of these results, it seems necessary to perform a comparative study of the structural and thermodynamic properties of the compounds occurring in the Cu-In and the Cu-Sn phase diagrams both at low and at high temperatures. Such study should also contribute to establish the effect of incorporating the third alloying element upon the stability to each of these binary phases. The general purpose of the present work is to explore the use of systematic *ab initio* calculations to characterize the Cu-In and Cu-Sn IPs and to establish reliable trends in the composition dependence of the structural, cohesive properties and EOS parameters in these key subsystems of the ternary Cu-In-Sn system. In the remainder of the present section we review the experimental and theoretical information on the Cu-In and Cu-Sn compounds and explain the specific aims of the work.

Various IPs have been detected in the Cu-In phase diagram, *viz.,* the -Cu_4In (cubic cI2), -Cu_9In_4 (cubic cP52), -Cu_7In_3 (triclinic aP40), -Cu_2In (superstructure based on hP6) and the $Cu_{11}In_9$ (monoclinic mC20) compound [4]. Although not included as a stable phase in the accepted Cu-In phase diagram, a tetragonal $CuIn_2$ (tI12) phase has been observed at low temperatures at the interface of Cu and In thin films [5] as well as in bulk Cu-In alloys [6]. In addition, a new phase described by the formula $Cu_{10}In_7$ with a monoclinic cell closely related to the $Cu_{11}In_9$ structure, has recently been found [7]. In the Cu-Sn system the following compounds have been detected: -$Cu_{17}Sn_3$ (cubic cI2), -Cu_4Sn (cubic cF16), -$Cu_{41}Sn_{11}$ (cubic cF416), -$Cu_{10}Sn_3$ (hexagonal hP26), -Cu_3Sn (orthorrombic oP80), -Cu_5Sn_4 (monoclinic mP36 and mC54) and ´-Cu_6Sn_5 (monoclinic mC44) [8]. The phase, which is a common equilibrium phase of both binary subsystems, presents equilibrium structures based on the B8 NiAs/Ni_2In family. At temperatures lower than 673 K the phase shows in the Cu-In-Sn phase diagram a region of continuous stability connecting the Cu-In and Cu-Sn subsystems [1]. The structure of the phase field in the Cu-In binary system has not yet been solved, although it is accepted that it involves at least a high temperature (HT) phase (´) and a low temperature (LT) one ( ), with a ´/ transition occurring at temperatures between 580 and 662 K depending upon composition [4]. The ´ structure is of the type $B8_2$ (hP6) with random partial occupation of the Cu sites with 2d symmetry, whereas the phase presents modulated superstructures based on the $B8_2$ – Ni_2In prototype, with an ordered distribution of defects, mainly vacancies, at sites (2d) [9,10]. In the Cu-Sn system the LT-η´ phase ("Cu_6Sn_5") and the HT-η phase ("Cu_5Sn_4") have monoclinic symmetry, with new

superstructures related to the NiAs-Ni_2In family of compounds [11]. In the Cu-Sn system the composition range of the η and η´ phase field is shifted towards higher contents of the alloying element (*viz.*, 45 at% Sn) compared with the Cu-In system (around 33 at%In).

Whereas the lattice-parameters (LPs) and molar volume (V_o) have been measured for the quoted Cu-In and Cu-Sn compounds, the bulk modulus (B_o), its pressure derivative (B_o') and other equation-of-state (EOS) parameters, as well as information on the electronic structure have been reported only for a few of these IPs. Considering this general lack of information, *ab initio* methods have been used to study some of the compounds of interest in this work. In particular, the present authors recently used DFT-GGA calculations to determine the LPs, V_o, B_o and B_o', the DOS and the energy of formation of the compounds $Cu_{10}In_7$, $Cu_{11}In_9$ and various "ideal" B8 NiAs/$InNi_2$ parent structures of the unknown equilibrium superstructures of the phase field in the Cu-In system [12]. Going one step further in this line of research, *ab initio* calculations based on the DFT-GGA and DFT-LDA are reported here for the following Cu-In compounds: -Cu_7In_3, -Cu_9In_4 and $CuIn_2$. Their structures are shown in Fig. 1. The first phase occurs as stable phase in the Cu-In phase diagram, and the second is stable only at high temperatures. The third phase has been observed in bulk Cu-In alloys [6] and thin films [5], and its treatment might be considered as first step in the modeling of the new Cu_2In_3Sn ternary compound recently found at 383 K by Liu *et al.* [13]. Moreover DFT-LDA calculations for the -Cu_2In, $Cu_{11}In_9$ and $Cu_{10}In_7$ compounds, recently studied by us using DFT-GGA [12], were performed. By combining the present *ab initio* results with those reported in Ref. [12] a comprehensive account of the thermodynamic, structural and electronic properties of most of the observed Cu-In intermetallics will be reported for the first time.

Some of the IPs occurring in the Cu-Sn phase diagram have been studied by other authors using *ab initio* techniques. Ghosh and Asta [14] determined the stability, phase transformations and elastic properties of the ´-Cu_6Sn_5 and -Cu_5Sn_4 phases by DFT calculations using ultrasoft pseudopotentials (US-PP). The calculated LPs, internal Wyckoff positions and B_o agree very well with the experimental results. Good agreement with experiments was also obtained for the energy of the ´/ transformation. Other results of their work will be referred to later in this section. Lee, Tan and Lim [15] determined the structural and elastic constants of ´-Cu_6Sn_5 single crystals using DFT calculations with the plane wave method, US-PP and the GGA approximation. The results were used to analyze the polycrystal stiffness on the basis of the single crystal properties, finding good agreement between the calculated Young´s modulus and experimental results. More recently, Zhow *et al.* [16] studied the structural, electronic and thermoelastic properties of ´-Cu_6Sn_5 using DFT calculations and the quasiharmonic approximation. Chen *et al*. [17] investigated the electronic origin of the anisotropic elastic properties of the superstructure Cu_3Sn. They found weak Sn-Cu bonding in Cu_3Sn suggesting that Sn atoms are the dominant diffusion species, a result that might be connected with the formation of vacancies and Kirkendall voids within the Cu_3Sn (oP80) superstructure. An *et al.* [18], using plane wave DFT calculations, US-PP and both GGA and LDA approximations, studied the elastic constants of the Cu_3Sn compound by considering a substructure of the (oP80) crystal structure. In the present work the following Cu-Sn compounds were treated using DFT-GGA: -Cu_4Sn and -$Cu_{10}Sn_3$ which have not yet been

theoretically studied; the -Cu_3Sn IP both in the orthorrombic (oP8) structure and the (oP80) superstructure; ´-Cu_6Sn_5 and two structural models for the -Cu_5Sn_4 phase, referred to as $_1$ (mP36) and $_2$ (mC54).

In Table 1 we summarize the crystallographic details of the Cu-In and Cu-Sn intermetallic phases studied here. The structural and crystallographic information needed in the present study was taken from [19].

Another purpose of the present work is to obtain new thermodynamic information of interest in understanding the phase formation systematics in Cu-In-Sn alloys [3] and modeling the ternary phase diagram [13]. To this end we perform *ab initio* calculations of the energy of formation of Cu-In and Cu-Sn compounds. The goals of this part of the work are the following. In the first place, we aim at critically determining to what extent DFT calculations are able to reproduce the available measurements of the energy of formation of the Cu-In and Cu-Sn compounds occurring as stable phases in the phase diagrams. In fact, Ghosh and Asta [14] recently reported a striking discrepancy between DFT calculations and experiments for the energy of formation of the ´ phase in the Cu-Sn system. In the present work we will extend such comparison to the remaining stable phases of the Cu-Sn phase diagram. Besides, we will present an analogous comparison for the stable phases of the Cu-In phase diagram, a critical study which has not yet been reported.

This work has also been motivated by the long-standing theoretical and practical interest in the comparison between *ab initio* results and the predictions of the phenomenological techniques developed to describe consistently the phase diagram and thermochemical data of alloys, which are usually referred to as the CALPHAD (*i.e.*, "Calculation of Phase Diagrams") method [20]. To this end, *ab initio* calculations have been performed for various IPs involved in the CALPHAD modeling of the stable-phase fields of the Cu-In-Sn phase diagram originated by incorporating Sn or In atoms into the intermetallics occurring in the Cu-In and Cu-Sn subsystems. These ternary IPs will be represented by the general two-sublattice formula $Cu_a(In,Sn)_b$, where the parentheses indicate that In and Sn substitute each other in the mixed sublattice. The Gibbs energy function of these two-sublattice phases is often formulated in the framework of the Compound Energy Formalism (CEF) [21]. When applying the CEF to the $Cu_a(In,Sn)_b$ intermetallics it is necessary to determine the thermodynamic properties of the Cu_aIn_b or Cu_aSn_b compounds, often called "end-members", which are generated by assuming that the sublattice in parentheses is fully occupied by In or by Sn, respectively. In Table 1 we summarize the end-members corresponding to various $Cu_a(In,Sn)_b$ schemes for the CEF modeling of the Cu-In-Sn system. In CALPHAD assessment work the thermodynamic properties of these stable or non-stable, hypothetical compounds are usually determined, in the so-called CALPHAD "optimization" procedure [22], by fitting the model expressions for Gibbs energy to the available experimental data. As an alternative, in the present work, the energy of formation of the end-members listed in Table 1 will be established by means of DFT – GGA calculations, and critically compared with the values obtained in a CALPHAD-type analysis of the Cu-In-Sn system [13].

2. Theoretical method

The present theoretical method has been described in Ref. [12]. Here we summarize only the main points. The total energy DFT calculations were performed using the projector augmented-wave method (PAW) [23] and

the VASP code [24], adopting the generalized gradient approximation due to Perdew and Wang (GGA-PW91) [25] for the exchange-correlation energy. In addition, calculations using the local density approximation (LDA) and the Ceperley and Alder [26] exchange-correlation potentials were performed for the Cu-In phases. The calculations were made by adopting a kinetic energy cut-off for the plane wave expansion of the electronic wavefunction of 314 eV. However, in order to test the effect of this choice upon the total energies and the energy of formation of the compounds (Section 3) calculations were performed using a cut-off energy of 450 eV for some selected compounds: Cu_3Sn (oP8), Cu_6Sn_5 (mC44) and Cu_7In_3 (aP40), and for the corresponding pure elements. While changes in the total energy are found to be less than 10 meV/atom (1 kJ/mol), we established that the energies of formation are converged within 2 meV/atom (0.2 kJ/mol) when adopting a cut-off energy of 314 eV.

For the PAWs we considered 11 valence electrons for Cu ($3d^{10}4s^1$), 3 for In ($5s^2p^1$) and 4 for Sn ($5s^2p^2$). We used Monkhorst-Pack k-point meshes [27] and the Methfessel-Paxton technique [28] with a smearing factor of 0.1 for the electronic levels. The convergence of the k-point meshes was checked until the energy has converged with a precision better than 1 meV/atom. For the Cu-In compounds studied in this work, the meshes of k points considered in the first Brillouin zones were 5x5x7 for Cu_7In_3, 7x7x7 for Cu_9In_4 and 13x13x15 for the $CuIn_2$-tI12. For the Cu-Sn compounds the k-point meshes were 9x9x9 for Cu_4Sn, 13x17x15 for Cu_3Sn (oP8), 13x1x17 for Cu_3Sn (oP80), 5x7x5 for ´-Cu_6Sn_5, 5x7x5 for $_1$-Cu_5Sn_4 and 5x9x7 for $_2$-Cu_5Sn_4. The maximum number of k points corresponds to the Cu_3Sn (oP8) phase with 720 k points in the irreducible Brillouin zone. The criterion for the self-consistent convergence of the total energy was 0.1 meV. The structures were optimized with respect to their LPs and the internal degrees of freedom compatible with the space group symmetry of the crystal structure until the forces were less than 20 meV/Å, and the energy variations with respect to the structural degrees of freedom was better than 0.1 meV.

The total energy (E) and external pressure (P) were calculated for values of volume (V) varying slightly around the equilibrium (up to 5%), relaxing all external and internal coordinates of the system. The bulk modulus (B_o) and its pressure derivative (B_o´) were obtained by fitting the calculated pressure-volume values to the P *vs*.V EOS due to Vinet *et al.* [29]. This equation is the one adopted in the literature to establish the EOS parameters of the elements (Section 3.1), in our previous *ab initio* work on Cu-In compounds [12] and in the work by Ghosh and Asta [14] on Cu-Sn compounds (Section 3.2). However, in order to test the effect of a different EOS upon the resulting B_o and B_o´ values, for the compound Cu_3Sn (oP8) we fitted the calculated data to the Birch-Murnaghan EOS [30]. Both models of EOS lead to almost the same results, the differences being only 0.1% for B_o and 6% for B_o´.

The energy of formation (EOF) of the IPs was calculated as

$$\Delta E^{\phi}(Cu_aM_b) = \frac{1}{a+b}E^{\phi}_{Cu_aM_b} - \left[\frac{a}{a+b}E^{\theta}_{Cu} + \frac{b}{a+b}E^{\psi}_{M}\right] \qquad Eq.1$$

where ΔE^{ϕ} is the energy of formation per atom of the Cu_aM_b (with M=In, Sn) compound with the structure , $E^{\phi}_{Cu_aM_b}$ the corresponding total energy, E^{θ}_{Cu} is the total energy per atom of Cu in its equilibrium phase (fcc),

and E_M^{ψ} is the total energy per atom of In or Sn in their equilibrium structure (= tI2 for In and tI4 for Sn, see below). This choice of the reference states allows a direct comparison of the theoretical ΔE^{ϕ} with the experimental values measured in calorimetric experiments and with the EOF values obtained in CALPHAD-type modeling of phase diagrams (Sections 3.4 and 3.5)

3. Results and discussion

In Table 2 we summarize the *ab initio* results for the elements Cu, In and Sn in their known equilibrium structures, *i.e.*, fcc for Cu, tI2 for In and tI4 for Sn. We report the LPs, V_o, B_o, and B_o'. In Tables 3 to 6 we present the calculated structural and EOS parameters for various stable, "ideal" B8 and hypothetical Cu-In and Cu-Sn phases.

3.1 Cohesive properties of the elements

The GGA results for Cu and In have been discussed elsewhere [12]. Here we will mention only the key points. For Cu the calculation overestimates the LP by 2%, but agrees with other theoretical values using the FP-LAPW [12] and US-PPs [14] approximations. The calculated B_o also agrees very well with the measured value. The theoretical B_o' is smaller than the experimental, but agrees with a reported US-PP value [14]. The present LDA calculation underestimates the LP of Cu by 2% and overestimates B_o by 30%.

The GGA calculated LPs of In agree within less than 2% with the experimental results at 291 K, and the calculated c/a ratio 1.524 compares very well with the experimental value 1.523. The calculation understimates B_o by about 13%, but yields a B_o' that agrees very well with the measured value [31]. As in the case of Cu, the LDA calculation underestimates the LPs of In by about 2%, and yields a c/a larger that the experimental one. In addition, B_o and B_o' are overestimated by 23% and 10%, respectively.

For Sn, only GGA calculations were performed. The lowest energy phase corresponds to the diamond structure, which is the most stable one at low temperature. The tetragonal tI4 phase is higher in energy than the diamond phase by 4.405 kJ/mol. The US-PP result by Ghosh and Asta [14], *viz.*, 4.557 kJ/mol is very close to our calculated energy difference. The calculated LPs parameters are larger than the experimental ones by approximately 2 %, whereas the *ab initio* c/a ratio is in very good agreement with the measured value. The calculation underestimates B_o by 16%, while B_o' lies between the experimental values. A comparison with the values reported by Ghosh and Asta [14] indicates an excellent agreement concerning the LPs. For B_o and B_o' the agreement is reasonably good, with differences of 6% and 16%, respectively.

3.2 Structural and EOS parameters for compounds

The structural and EOS parameters for the Cu-In and Cu-Sn compounds studied in the present work are compared in Tables 3 and 4, respectively, with experimental data theoretical results from the literature. The unit cell internal coordinates of Cu-In and Cu-Sn compounds calculated in the present work are listed in Tables 5 and 6, respectively.

The GGA calculated LPs for Cu-In compounds deviate positively from experiments by less than 1.5%. A similar good agreement was found for other Cu-In compounds in our previous PAW and FP-LAPW [12] work. The LDA values are smaller than the experimental ones by less that 3%. The GGA calculated LP values for the -$Cu_{10}Sn_3$, -Cu_3Sn, ´-Cu_6Sn_5, $_1$-Cu_5Sn_4 and $_2$-Cu_5Sn_4 intermetallics (Table 4) agree with the available measurements within less than 3%. For the -Cu_3Sn (oP80) superstructure the calculated LPs agree within 1% with those predicted by Chen *et al.* [17] using a similar *ab initio* calculation but considering a different GGA functional. Larger discrepancies are found when comparing the present LPs for the (oP8) structure with the *ab initio* US-PP values obtained by of An *et al.* [18], using the same PW91 exchange correlation functional used in this work, a larger cut-off energy and a lower number of k points (up to 80). The present B_o values for the -Cu_3Sn compound both in the (oP8) and the (oP80) structures are about 30 % smaller than the polycrystalline average bulk modulus obtained from the single crystal elastic constants, reported by An *et al.* [18] and Chen *et al.* [17], respectively. For the phases, the present LPs as well as B_o and B_o´ values agree very well with the corresponding *ab initio* ones reported by Ghosh and Asta [14].

In Fig. 2 (a) to (d) we plot, using filled symbols, the present GGA and LDA results. Empty circles and triangles are used to represent the calculated results from Refs. [12] and [14], respectively. Crosses represent experimental values. The dotted lines are only to guide the eye.

The comparisons with experiments in Fig. 2(a) indicate that the present GGA calculations systematically overestimate V_o of the stable Cu-In and Cu-Sn compounds, as found for other systems (see, *e.g.*, Refs. 32, 33). The LDA calculated V_o values for the same phases are smaller than the experimental ones with a more important discrepancy. A similar behavior has been found for other intermetallic systems [34-36]. No LDA calculations were performed in the present work to compare with the GGA results for Cu-Sn compounds. However, the results by Ghosh and Asta [14] for some of the IPs included in Fig. 2(b) indicate that the relation between GGA and LDA values for V_o of the Cu-Sn phases is analogous to that found by us for Cu-In compounds.

The present V_o values for Cu-In phases, together with most of those from Ref. [12] (Fig. 2(a)) as well as the present values for Cu-Sn compounds (Fig. 2(b)) indicate a smooth variation with composition. The GGA values from Ref. [12] deviating positively from the general trend in Fig. 2(a) correspond to the "ideal" CuIn-$B8_1$ and $CuIn_2$-$B8_2$. It should be emphasized that these "ideal" phases are not stable in the Cu-In phase diagram.

Most of the B_o values for Cu-In (Fig. 2(c)) and Cu-Sn (Fig. 2(d)) compounds also indicate a smooth variation with composition. The few values deviating negatively from the general trends correspond to the "ideal" Cu_2In and $CuIn_2$ intermetallics treated in Ref. [12], the "ideal" Cu_2Sn and $CuSn_2$ phases studied here and in [14], and the -Cu_4Sn phase which is stable only at high temperatures in the Cu-Sn phase. Anticipating the results in Section 3.4, it may be remarked that these "ideal" compounds, which are not stable in the Cu-In or Cu-Sn phase diagrams, and the -Cu_4Sn phase which occurs only at high temperatures, are correctly predicted by the present calculations as unstable with respect to the constituent elements at 0 K.

Finally, the results in Fig. 2 indicate that the *ab initio* calculated V_o and B_o for the Cu-In and Cu-Sn compounds deviate negatively from those given by a linear interpolation between the values for the elements. It has been remarked that a negative deviation from linearity in the composition dependence in V_o (or B_o) does not necessarily imply a positive deviation in B_o (or V_o), as generally expected [35]. The present results support this observation.

3.3 Electronic structure of intermetallic phases

In Fig. 3 we plot the DOS for the Cu_7In_3, $Cu_{11}In_9$ and $CuIn_2$ phases of the Cu-In system, and in Fig. 4 the ones for the $Cu_{10}Sn_3$, Cu_3Sn and Cu_6Sn_5 phases of the Cu-Sn system. The partial DOS of electrons Cu-d, Cu-s, Cu-p and In/Sn s and p are also plotted.

The DOS per atom (given in states eV^{-1} $atom^{-1}$) at the Fermi level is relatively low but finite in all cases, indicating metallic character. It increases slightly with the In and Sn content for the Cu-In and Cu-Sn compounds, respectively. In all the cases the DOS present similar characteristics. As found in Ref. [12], the most prominent bonding band is completely occupied and extends from -5 to -2.5 eV approximately below the Fermi level. It is mostly defined by the contribution of Cu-d states, with additional minor contributions of In (or Sn) s and p states for Cu-In (or Cu-Sn) compounds. The main bonding mechanism in these systems comes from the interaction between transition metal nearest neighbours, as found recently in other related systems like Cu-Al [37], Ni-In [36] and Ni-Sn intermetallics [35]. As the content of In and Sn increases in the compounds the width of the main band reduces, which is a combined effect of the reduction in the number of Cu-Cu nearest neighbors (NN) and changes in the Cu-Cu nearest-neighbor interatomic distances (NND), as shown in Table 7. These values may be compared with two characteristic distances in the Cu fcc lattice, *viz.*, the Cu-Cu nearest-neighbor distance (2.57 Å), and that between first and second neighbours (≈3 Å).

For the Cu-In system, at energies between -10 to -6 eV approximately, the DOS have free electron character, determined mainly by the overlapped contributions of the Cu-4s and In-5s states. At the lowest energies the In-s and Cu-s partial DOS have the typical free-electron parabolic shape. In the whole range of energies plotted, there is superposition of the 3d, 4s and 4p states of Cu. However the relative contribution of Cu 4s and 4p is minor and reduces as the In content is increased. The contribution of the In-5p states is relevant at higher energies (-6 eV approximately for Cu_7In_3, shifting to higher energies for increasing In content), becoming more important in a region in which the In-5s states decay. There is overlap between In-5p and Cu-3d indicating hybridization effects between these electronic states in the Cu-In bonds. The main bonding band shifts slightly to lower energies with increasing In content.

Similar characteristics are found for the DOS of the Cu-Sn compounds (Fig. 4). However, more structured DOS showing the presence of many more resonance peaks, as compared to the Cu-In ones, are observed in the main bonding band. The contribution of Cu s and p states as well as Sn s and p states shift to lower energies. Since hybridization effects between Sn-5p states and Cu-3d states contribute to the bonding mechanism, the fact that Sn has one more p electron in its atomic electronic configuration as compared to In, might in principle explain why the cohesion is always stronger for the Cu-Sn compounds than for the Cu-In ones.

3.4 Energy of formation of compounds

The energy of formation from the elements (EOF) of the Cu-In and Cu-Sn compounds studied in the present work are compared in Tables 8 and 9 with other experimental and theoretical information. In Fig. 5 the composition dependence of the EOF values for the Cu-In (Fig. 5(a)) and Cu-Sn (Fig. 5(b)) systems is presented. Filled symbols correspond to phases stable at low temperature ("LT") in the phase diagram; empty symbols to phases stable only at high temperatures ("HT") and half-filled symbols to "ideal" B8 parent structures in the Cu-In [12] and Cu-Sn system.

In agreement with the fact that the Cu-In compounds treated in the present work are stable at low temperatures in the Cu-In phase diagram, they are predicted as thermodynamically stable with respect to the elements Cu and In (Fig. 5 (a)). The calculated EOF of the Cu_9In_4 phase is positive. This result is also compatible with the phase diagram [4] because the Cu_9In_4 compound is stable only at high temperatures, *i.e.*, its thermodynamic stability is expected to depend also upon the entropy contribution to Gibbs energy. The present results also predict that the $CuIn_2$ (tI12) phase is thermodynamically stable with respect to the pure elements. This phase is not included as a stable phase in the accepted Cu-In phase diagram, but has been detected at the interface of thin films of Cu and In, as well as in bulk Cu-In alloys at low temperatures. A similar qualitative agreement with the phase diagram is obtained for the Cu-Sn compounds (Fig. 5(b)): the calculated EOF is negative for the phases occurring at low temperatures and for the Cu_5Sn_4 phase, but positive for the compounds $Cu_{10}Sn_3$ and Cu_4Sn, which are stable at high temperature. For the two structural forms of the -Cu_3Sn phase considered here, the oP8 structure and the oP80 superstructure, the present calculations indicate that the first one is relatively more stable than the second one by only 0.14 kJ/mol. In addition, the oP80 superstructure, which is expected to be the best structural description of the phase, is predicted as thermodynamically unstable with an EOF of 0.07 kJ/mol. A possible explanation for this unexpected result is the role that partially and randomly occupied sites could be playing on the stabilization of the actual phase, a problem that has not been studied in the present work. In fact, for the present *ab initio* calculation we have considered fully 4c Sn occupied sites, while strictly speaking the available structural data suggest partial 0.98 Sn and 0.02 Cu occupation for sites 4c (j) with j = 1-5.

In agreement with that fact that the "ideal" B8 structures are not stable in the Cu-In [12] or the Cu-Sn phase diagrams the present calculations yield positive values for EOF, *i.e.*, these compounds are predicted as thermodynamically unstable with respect to the constituent elements. The only exception is the "ideal" CuSn phase, which in fact, presents the lowest EOF value obtained by us for Cu-Sn compounds (Fig.5 (b)). This prediction is in very good agreement with previous calculations by Ghosh and Asta [14].

A key finding of the present work is the existence of significative positive differences between the *ab initio* calculated EOF and those measured in the Cu-In (Table 8) and Cu-Sn (Table 9) systems. A difference of the order of 4 kJ/mol between the GGA calculated and the experimental EOF for the ´-Cu_6Sn_5 has previously been reported by Ghosh and Asta [14]. In the present work such discrepancy has been corroborated and, in addition, comparable positive differences have been found for the remaining stable phases of the Cu-Sn phase

diagram. Moreover, since the quoted calorimetric data have been used as input in CALPHAD work, differences of the same order of magnitude have been established between the GGA values for Cu-Sn compounds and those produced in CALPHAD assessments.

Ghosh and Asta [14] also found that the agreement between theoretical and experimental EOF for some Cu-Sn IPs is better when the LDA is adopted, which is not the usual case. In view of this result, both GGA and LDA calculations were performed for the Cu-In compounds, with the following results. With the GGA, positive differences up to 7.4 kJ/mol are found between the calculated EOF and those determined calorimetrically. When adopting the LDA the difference decreases by approximately 2.6 kJ/mol, which represents a reduction of 35 to 62% in the difference with experiments.

Various aspects of the present findings will be discussed. Concerning the experimental EOF values, it should be emphasized that the current database for the Cu-In system includes high-temperature calorimetric data from various sources, mainly for In contents lower than about 40at%. In particular, for alloys with 20 < at%In < 30 the data show considerable discrepancies, with an experimental scatter band of about 2 kJ/mol [38]. Moreover, the experimental data does not allow a critical test of the location of the minimum in the EOF *vs.* composition relation. According to Fig. 5(a), in the absence of EOF information for the actual (*i.e.*, not the "ideal") -phase, the minimum is placed at the composition corresponding to the $Cu_{10}In_7$ compound, both for the GGA and LDA calculations.

Concerning the theoretical implications of the present results, it may be noted that in the field of the CALPHAD modeling of the phase diagrams [see, *e.g.*, Refs. 39, 40] various attempts have been made in the last decades to understand the disagreement between *ab initio* and structural energy differences ("lattice-stabilities") between the bcc and the fcc (or hcp) phases of the elements [40]. On the other hand, comparisons between theoretical and experimental (or CALPHAD generated) EOFs have been reported only for a few binary systems [see, *e.g.*, Refs. 14, 34, 35]. This lack of information motivates us to perform various attempts to gain additional insight on the differences found in the Cu-In and Cu-Sn systems, by using two complementary approaches. The first approach aims at obtaining and comparing *ab initio* and experimental EOF values for stable compounds in binary systems closely related to the Cu-In and Cu-Sn, and to establish trends across the Periodic Table. In particular, we have studied *ab initio* the EOF of various stable Ni-In and Ni-Sn compounds. Our calculations, which will be presented elsewhere, also show systematic differences with the experimental EOFs, although smaller than the present ones [41].

3.5 Relative thermodynamic stability of compounds

The second, complementary approach to characterize the difference between *ab initio* and experimental values, involves comparisons of the present results with other thermodynamic quantities introduced in the following, which account for the relative thermodynamic stability of related compounds.

In the first place, using the EOF values obtained in the present work we calculate the energy difference $\Delta(\Delta E^{\phi}(\eta_1 / \eta')) = \Delta E^{\phi}(\eta_1) - \Delta E^{\phi}(\eta')$ between the EOF of the $_1$ and ´ structures of the Cu-Sn system, which might be considered as an approximation to the energy difference measured upon the actual phase

transition [14, 42]. In this way we get $\Delta(\Delta E^{\phi}(\eta_1/\eta'))$ = 0.389 kJ/mol. This value falls within the experimental scatter band determined by the measurements performed on heating (represented as 0.396 kJ/mol < $\Delta(\Delta E^{\phi}(\eta_1/\eta'))$ < 0.450 kJ/mol) and those obtained on cooling (represented as 0.276 kJ/mol < $\Delta(\Delta E^{\phi}(\eta_1/\eta'))$ < 0.396 kJ/mol) [14]. We also obtain $\Delta(\Delta E^{\phi}(\eta_2/\eta'))$ = 0.740 kJ/mol. The present $\Delta(\Delta E^{\phi}(\eta_1/\eta'))$ and $\Delta(\Delta E^{\phi}(\eta_2/\eta'))$ values agree well with those reported by Ghosh and Asta [14], *viz.*, 0.321 kJ/mol and 0.610 kJ/mol, respectively.

Secondly, comparisons will be performed with analogous EOF differences concerning other phases in the Cu-In-Sn present system. For the energy difference between the and phases of the Cu-In system we estimate $\Delta(\Delta E^{\phi}(\gamma/\delta))$=1.45 kJ/mol, which compares reasonably well with the experimental [43] result $\Delta(\Delta E^{\phi}(\gamma/\delta))$=1.95 kJ/mol. Another phase transition occurring in the -phase field of the Cu-In system has been reported [6] but the complex structures involved have not yet been established, and therefore could not be treated in the present work.

Finally, the *ab initio* predictions will be used to determine the difference $\Delta(\Delta E^{\phi}(Cu_aM_b)) = \Delta E^{\phi}(Cu_aSn_b) - \Delta E^{\phi}(Cu_aIn_b)$ expressing the relative stability of two compounds with the same stoichiometry and structure (ϕ), one from the Cu-Sn system (in general, Cu_aSn_b) and the other from the Cu-In system (Cu_aIn_b). The theoretical values for this EOF difference will be compared with information obtained from the CALPHAD analysis of the Cu-In-Sn phase diagram reported by Liu *et al*. [13]. In their work, based upon the Compound Energy Formalism (CEF), a two-sublattice scheme of the type $Cu_a(In, Sn)_b$ was adopted to model the -$Cu_7(In,Sn)_3$ and -$Cu(In,Sn)_3$ phases, as well as other compounds not included in the present study, *viz.*, the $Cu_{41}(In,Sn)_{11}$ intermetallic from the Cu-Sn system [8] and the $Cu_{77}(In,Sn)_{23}$ compound detected only in ternary alloys [1]. Using the thermodynamic parameters reported by Liu et *al*. [13] the differences $\Delta(\Delta E^{\phi}(Cu_aM_b))$ between the EOFs of the Cu_aSn_b and Cu_aIn_b "end-member" compounds were evaluated by us, and compared with the GGA $\Delta(\Delta E^{\phi}(Cu_aM_b))$ differences obtained in the present work (Fig. 6). In this figure filled circles and squares correspond to phases stable at low-temperature (LT) in the Cu-In and Cu-Sn systems, respectively. Open circles and squares correspond to high temperature (HT) phases of the Cu-In and Cu-Sn systems, respectively. Filled triangles represent the $\Delta(\Delta E^{\phi}(Cu_aM_b))$ differences obtained from the thermodynamic parameters for -$Cu_7(In,Sn)_3$ and -$Cu_3(In,Sn)$ compounds reported in Ref. [13]. For comparisons with the theoretical trends, the $\Delta(\Delta E^{\phi}(Cu_aM_b))$ differences corresponding to the $Cu_{41}(In,Sn)_{11}$ and $Cu_{77}(In,Sn)_{23}$ compounds are also included using empty triangles. Figure 6 suggests a general good agreement between the *ab initio* calculated $\Delta(\Delta E^{\phi}(Cu_aM_b))$ values and those obtained from a thermodynamic description of the Cu-In-Sn system based on the CEF. This result, together with the previous comparisons in the present section lend support to the belief that the present *ab initio* treatment accounts well for the direct and indirect information available upon the relative stability of Cu-In and Cu-Sn compounds.

4. Summary and conclusions

The recent experimental work on Cu-In-Sn lead-free soldering open up the need for information on trends in the relevant cohesive and thermodynamic properties of the binary IPs occurring in the Cu-In and the Cu-Sn phase diagrams both at low and at high temperatures. The present work reports a comparative study of the Cu-In and Cu-Sn compounds using density-functional-theory calculations. Using the projector augmented wave method and the exchange and correlation functions of Perdew and Wang in the generalized gradient approximation (GGA), we have established the lattice-parameters (LPs), molar volume (V_o), bulk modulus (B_o) and its pressure derivative (B_o'), the electronic density of states (DOS) and the energy of formation (EOF) from the elements of the -Cu_7In_3 (aP40), -Cu_9In_4 (cP52) and $CuIn_2$ (tI12) Cu-In compounds, and -Cu_4Sn (cF16), -$Cu_{10}Sn_3$ (hP26), -Cu_3Sn both in the (oP8) structure and the (oP80) superstructure, ´-Cu_6Sn_5 (mC44) and -Cu_5Sn_4 both in the $_1$ (mP36) and $_2$ (mC54) structural forms. In addition, various hypothetical structures obtained by replacing In (or Sn) by Sn (or In) are studied, because of their relevance in CALPHAD modeling of the Cu-In-Sn phase diagram he Cu-In compounds occurring in the phase diagram, were also treated using the local-density-approximation (LDA) with the Ceperley and Alder exchange and correlation potentials. The key results of the work are the following.

The GGA calculations systematically overestimate V_o of the stable Cu-In and Cu-Sn compounds. The LDA calculated V_o values for the Cu-In phases are smaller than the experimental with a more important discrepancy. The V_o results for Cu-In and Cu-Sn indicate a smooth variation with composition. Only the GGA values for the "ideal" CuIn-$B8_1$ and $CuIn_2$-$B8_2$, which are not stable in the Cu-In phase diagram, deviate positively from the general trend. The calculated B_o values also vary smoothly with composition, with the only exception of the GGA results for the "ideal" B8 Cu_2In, $CuIn_2$, Cu_2Sn and $CuSn_2$, as well as the -Cu_4Sn phase which is stable only at high temperature in the Cu-Sn phase diagram. Both the V_o *vs.* composition and B_o *vs.* composition relations exhibit negative deviations from the linearity.

The calculated DOS of the Cu-In and Cu-Sn compounds indicate that all phases included in the present work present metallic behavior. Their calculated DOS show similar characteristics. The most prominent bonding band is mostly determined by the contribution of Cu-d states, with additional minor contributions of the In (or Sn) s and p states for Cu-In (or Cu-Sn) compounds. The main bonding mechanism in these systems comes from the interaction between Cu-Cu nearest neighbours. As the content of In and Sn in the compounds increases, the width of the main band reduces, in correlation with the reduction of the number of Cu-Cu bonds and changes in the nearest-neighbor distances. The calculated DOS for Cu-In and Cu-Sn compounds shows the overlap between In (or Sn) 5p and Cu-3d indicating that hybridization effects also contribute to the bonding mechanism. The fact that Sn has one more p electron than In in its atomic electronic configuration, might explain why the cohesion is always stronger in the Cu-Sn compounds than in the Cu-In ones.

The Cu-In and Cu-Sn compounds observed at low temperatures in the phase diagrams are predicted by the EOF calculations as thermodynamically stable with respect to the elements Cu and In (or Sn). The $CuIn_2$ (tI12) phase observed in thin films and in bulk Cu-In alloys, is also predicted to be thermodynamically stable.

The calculated EOF for the Cu_9In_4, $Cu_{10}Sn_3$ and Cu_4Sn, which are observed only at high temperatures, is positive, suggesting that its thermodynamic stability depends upon the entropy contribution to Gibbs energy. The "ideal" B8 structures, which are not stable in the phase diagrams, are predicted as thermodynamically unstable both in the Cu-In and in the Cu-Sn systems, with the exception of the CuSn phase.

The *ab initio* calculated EOF values for Cu-In and Cu-Sn compounds show a positive difference with the calorimetric data. For Cu-In compounds differences up to 7.4 kJ/mol are found betweeen the GGA calculated EOF and the experimental values. If the LDA is adopted the difference with experiments decreases by 35 to 62%. The present results corroborate previous findings by Ghosh and Asta in the Cu-Sn system [14], by Ghosh in the Ni-Sn system [35] and by Ramos de Debiaggi *et al.* [41] in the Ni-In and Ni-Sn system.

Various quantities involving differences between the EOF of compounds have been considered. In particular, we studied the energy differences between the and ´ structures of the Cu-Sn system and the and phases of the Cu-In system. The theoretical values agree well with the experimental values. We also evaluate the EOF difference between two compounds with the same stoichiometry and structure, one from the Cu-Sn system and the other from the Cu-In system. The theoretical energy differences are shown to compare very well with the values from a CALPHAD-type modeling of the Cu-In-Sn phase diagram. It is suggested that the *ab initio* generated EOF differences could be used as a complement in the CALPHAD modeling of ternary and higher-order phase diagrams, in particular, when the necessary experimental data are scarce, unreliable or lacking.

Acknowledgements

This work was supported by Agencia Nacional de Promoción Científica y Tecnológica (BID 1728/OC-AR, PICT-2006 1947), Universidad Nacional del Comahue (Project I157) and Universidad Nacional de Cuyo (SeCTyP, Project 1873). One of the authors (SRD) wish to thank Dr. V. Ganduglia Pirovano, from Instituto de Catálisis y Petroquímica – CSIC, for helpful suggestions concerning the VASP calculations; Dr. R. Faccio, from Universidad de la República (Uruguay) and Dr. O. Piro from Universidad Nacional de La Plata (Argentina) for their helpful comments on the symmetry properties of the modeled Cu_3Sn phase.

References

[1] W. Köster, T. Gödecke, D. Heine, The constitution of the Copper-Indium-Tin System, Z. Metallkd. 63 (1972) 802-807.

[2] S.A. Sommadossi, Investigation on diffusion soldering in Cu/In/Cu and Cu/In48Sn/Cu systems, Dissertation an der Universität Stuttgart, Bericht Nr. 125, 2002.

[3] S.A. Sommadossi, A. Fernández Guillermet, Interface reaction systematics in the Cu/In48Sn/Cu system, Intermetallics 15 (2007) 912-917.

[4] H. Okamoto, Comment on Cu-In (Copper-Indium), J. Phase Equilib. 15 (1994) 226-227.

[5] W. Keppner, T. Klas, W. Körner, R. Wesche, G. Schatz, Compound formation at Cu-In thin-film interfaces detected by perturbed - angular correlations, Phys. Rev. Lett. 54 (1985) 2371-2374.

[6] A. Bolcavage, S.W. Chen, C.R. Kao, Y.A. Chang, A.D. Romig Jr, Phase equilibria of the Cu-In system I: experimental investigation, J. Phase Equilib. 14 (1993) 14-21.

[7] S. Piao, S. Lidin, A new compound in the Cu-In system - the synthesis and structure of $Cu_{10}In_7$, Z. Anorg. Allg. Chem. 634 (2008) 2589-2593.

[8] N. Saunders, A.P. Miodownik, The Cu-Sn (Copper-Tin) system, J. Phase Equilib. 11 (1990) 278-287.

[9] S. Lidin, A.K. Larsson, A survey of superstructures in intermetallic NiAs-Ni_2In-type phases, J. Solid State Chem. 118 (1995) 313-322.

[10] M. Elding-Pontén, L. Stenberg, S. Lidin, The -phase field of the Cu-In system, J. Alloys Compd. 261 (1997) 162-171.

[11] A.K. Larsson, L. Stenberg, L. Lidin, The superstructure of domain-twinned '-Cu_6Sn_5, Acta Crystallogr. B 50 (1994) 636-643; A.K. Larsson, L. Stenberg, S. Lidin, Crystal structure modulation in –Cu_5Sn_4, Z. Kristallogr. 210 (1995) 832-837.

[12] S. Ramos de Debiaggi, G.F. Cabeza, C. Deluque Toro, A.M. Monti, S. Sommadossi, A. Fernández Guillermet, *Ab initio* study of the structural, thermodynamic and electronic properties of the $Cu_{10}In_7$ intermetallic phase, J. Alloys Compd. 509 (2011) 3238-3245.

[13] X.J. Liu, H.S. Liu, I. Ohnuma, R. Kainuma, K. Ishida, S. Itabashi, K. Kameda, K. Yamaguchi, Experimental determination and thermodynamic calculation of the phase equilibria in the Cu-In-Sn system, J. Elect. Mater. 30 (2001) 1093-1103.

[14] G. Ghosh, M. Asta, Phase stability, phase transformations, and elastic properties of Cu_6Sn_5: *Ab initio* calculations and experimental results, J. Mater. Res. 20 (2005) 3102-3117.

[15] N.T.S. Lee, V.B.C. Tan, K.M. Lim, First-principles calculation of structural and mechanical properties of Cu_6Sn_5, Appl. Phys. Lett. 88 (2006) 031913.

[16] W. Zhou, L. Liu, P. Wu, Structural, electronic and thermo-elastic properties of Cu_6Sn_5 and Cu_5Zn_8 intermetallic compounds: First-principles investigation, Intermetallics 18 (2010) 922-928.

[17] J. Chen, Y. Lai, Ch. Ren, D. Huang, First-principles calculations of elastic properties of Cu_3Sn superstructure, Appl. Phys. Lett. 92 (2008) 081901.

[18] R. An, Ch. Wang, Y. Tian, H. Wu, Determination of the elastic properties of Cu_3Sn through first-principles calculations, J. Elect. Mater. 37 (2008) 477-482.

[19] P. Villars, Pearson´s Handbook Desk Edition, ASM International, Materials Park, Ohio, 1997.

[20] L. Kaufman, H. Bernstein, Computer Calculation of Phase Diagrams, Academic Press, New York, 1970.

[21] M. Hillert, The compound energy formalism, J.Alloys Compd. 320 (2001) 161-176.

[22] Fernández Guillermet, Assessment of phase stability and thermochemistry of high-melting alloys and compounds: a systematic approach based on Gibbs energy modelling, in: K.E. Spear (Ed.), Proc. Nineth International Conference on High Temperature Materials Chemistry, The Electrochemical Society Proceedings Vol. 97, Pennington, New York, 1997, pp. 135-144.

[23] P.E. Blöchl, Projector augmented-wave method, Phys. Rev. B 50 (1994) 17953-17979; G. Kresse, J. Joubert, From ultrasoft pseudopotentials to the projector augmented-wave method, Phys. Rev. B 59 (1999) 1758-1775.

[24] G. Kresse, J. Furthmüller, Efficiency of *ab-initio* total energy calculations for metals and semiconductors using a plane-wave basis set, Comput. Mater. Sci. 6 (1996) 15-50.

[25] J.P. Perdew, Y. Wang, Accurate and simple analytic representation of the electron-gas correlation energy, Phys. Rev. B 45 (1992) 13244-13249.

[26] D.M. Ceperley, B.J. Alder, Ground state of the electron gas by a stochastic method, Phys. Rev. Lett. 45 (1980) 565-569.

[27] H.J. Monkhorst, J.D. Pack, Special points for Brillouin-zones integrations, Phys. Rev. B 13 (1976) 5188-5192.

[28] M. Methfessel, A.T. Paxton, High-precision sampling for Brillouin-zone integration in metals, Phys. Rev. B 40 (1986) 3616-3621.

[29] P. Vinet, J.H. Rose, J. Ferrante, J.R. Smith, Universal features of the equation of state of solids, J. Phys.: Condens. Matter 1 (1989) 1941-1963.

[30] F. Birch, Finite elastic strain of cubic crystals, Phys. Rev. 71 (1947) 809-824.

[31] K. Takemura, Effect of pressure on the lattice distortion of indium to 56 GPa, Phys. Rev. B 44 (1991) 545-549.

[32] M. Fuchs, J.L.F. Da Silva, C. Stampfl, J. Neugebauer, M. Scheffler, Cohesive properties of group-III nitrides: A comparative study of all-electron and pseudopotential calculations using the generalized gradient approximation, Phys. Rev. B. 65 (2002) 24512.

[33] J.L.F. Da Silva, C. Stampfl, M. Scheffler, Converged properties of clean metal surfaces by all-electron first-principles calculations, Surf. Sci. 600 (2006) 703-715.

[34] G. Ghosh, M. Asta, First-principles calculation of structural energetics of Al–TM (TM = Ti, Zr, Hf) intermetallics, Acta Mater. 53 (2005) 3225–3252.

[35] G. Ghosh, First-principles calculation of phase stability and cohesive properties of Ni-Sn intermetallics, Metall. Mater. Trans. A 40 (2009) 4-23.

[36] C.E. Deluque Toro, S. Ramos de Debiaggi, A.M. Monti, Study of Cohesive, Electronic and Magnetic Properties of the Ni-In Intermetallic System, Phys. B (2012). http://dx.doi.org/10.1016/j.physb.2011.12.075. In press.

[37] W. Zhou, L. Liu, B. Li, Q, Song, P. Wu, Structural, elastic and electronic properties of Al-Cu intermetallics from first-principles calculations, J. Elect. Mater. 38 (2008) 356-364.

[38] C.R. Kao, A. Bolcavage, S.-L. Chen, S.W. Chen, Y.A. Chang, A.D. Romig Jr., Phase equilibria of the Cu-In system II: thermodynamic assessment and calculation of phase diagram, J. Phase Equilib. 14 (1993) 22-30.

[39] P.E.A. Turchi, I. A. Abrikosov, B. Burton, S.G. Fries, G. Grimvall, L. Kaufman, P. Korzhavyi, V. Rao Manga, M. Ohno, A. Pisch, A. Scott, W. Zhang, Interface between quantum-mechanical-based approaches,

experiments, and CALPHAD methodology, CALPHAD: Comput. Coupling Phase Diagrams Thermochem. 31 (2007) 4–27.

[40] Y. Wang, S. Curtarolo, C. Jiang, R. Arroyave, T. Wang, G. Ceder, L.-Q. Chen, Z.-K. Liu, *Ab initio* lattice estability in comparison with CALPHAD lattice stability, CALPHAD: Comput. Coupling Phase Diagrams Thermochem. 28 (2004) 79–90.

[41] S. Ramos de Debiaggi, C. Deluque Toro, G. Cabeza, A. Fernández Guillermet, Thermodynamic properties of M-In-Sn (M = Cu, Ni) intermetallics: *ab initio* database and systematics, unpublished.

[42] A. Gangulee, G.C. Das, M.B. Bever, An x-ray diffraction and calorimetric investigation of the compound Cu_6Sn_5, Metall. Trans. 4 (1973) 2063-2066.

[43] Z. Bahari, E. Dichi, B. Legendre, Heat content and heat capacity of $Cu_{0.7}In_{0.3}$ from 298 K to 1273 K, Z. Metallkd. 90 (1999) 55-59.

[44] M.E. Straumanis, L.S. Yu, Lattice parameters, densities, expansion coefficients and perfection of structure of Cu and Cu-In alpha phase, Acta Crystallogr. A 25A (1969) 676-682.

[45] M. Kamtola, E. Tokola, X-ray studies on the thermal expansion of copper-nickel alloys, Phys. 223A (1967) 1-10.

[46] W.C. Overton Jr., J. Gaffney, Temperature variation of the elastic constants of cubic elements, Phys. Rev. 98 (1955) 969-977.

[47] D.J. Steinberg, Some observations regarding the pressure dependence of the bulk modulus, J. Phys. Chem. Solids 43 (1982) 1173-1175.

[48] J.A. Rayne, B.S. Chandrasekhar, Elastic constants of tin from 4.2 K to 300 K, Phys. Rev. 120 (1960) 1658-1663.

[49] H.S. Liu, H.S. Liu, X.J. Liu, Y. Cui, C.P. Wang, I. Ohnuma, R. Kainuma, Z.P. Jin, K. Ishida, Thermodynamic assessment of the Cu-In binary system, J. Phase Equilib. 23 (2002) 409-415.

[50] E. Dichi, B. Legendre, Enthalpy of formation of $Cu_{0.7}In_{0.3}$ and $Cu_{0.64}In_{0.36}$ phase by solution calorimetry, Z. Metallkd. 91 (2000) 47-50.

[51] T. Kang, H.V. Kehaiain, R. Castanet, Themodynamic study of the Copper-Indium binary system. I. Calorimetric study, J. Calorim. Anal. Therm. 7 (1976) 1-14.

[52] J.-H. Shim, Ch.-S. Oh, B.-J. Lee, D.N. Lee, Thermodynamic assessment of the Cu-Sn system, Z. Metallkd. 87 (1996) 205-212.

[53] H. Flandorfer, U. Saeed, C. Luef, A. Sabbar, H. Ipser, Interfaces in lead-free solder alloys: enthalpy of formation of binary Ag-Sn, Cu-Sn and Ni-Sn intermetallic compounds, Thermochim. Acta 459 (2007) 34-39.

[54] K.W. Moon, W.J. Boettinger, U.R. Kattner, F.S. Bianchello, C.A.Handwerker, Experimental and thermodynamic assessment of the Sn-Ag-Cu system, J. Elect. Mater. 29 (2000) 1122-1136.

[55] X.J. Liu, C.P. Wang, I. Ohnuma, R. Kainuma, K. Ishida, Experimental investigation and thermodynamic calculation of the phase equilibria in the Cu-Sn annd Cu-Sn-Mn systems, Metall. Mater. Trans. 35A (2004) 1641-1654.

Figure captions

Fig. 1: Structures of the Cu-In and Cu-Sn intermetallic phases calculated in the present work: a) δ-Cu_7In_3 (aP40; 30 at%In), b) -Cu_9In_4 (cP52; 30 at%In), c) $CuIn_2$ (tI12; 67 at% In), d) -Cu_4Sn (cF16; 20 at% Sn), e) -$Cu_{10}Sn_3$ (hP26; 23 at% Sn), f) -Cu_3Sn (oP8; 25 at% Sn), g) -Cu_3Sn (oP80; 25 at% Sn), h) $_1$-Cu_5Sn_4 (mP36; 44 at% Sn) i) $_2$ -Cu_5Sn_4 (mC54; 44 at% Sn) and j) ´-Cu_6Sn_5 (mC44; 45 at% Sn) structures. Dark grey, light grey and black spheres represent Cu, Sn and In atoms respectively.

Fig. 2: Thermophysical properties of the Cu-In and Cu-Sn intermetallic phases calculated in the present work as functions of the atomic concentration of In and Sn: (a and b) the volume (V_o) per atom; (c and d) bulk modulus (B_o). Filled symbols correspond to values calculated in this work; empty circles to GGA results from Ref. [12]; empty triangles to GGA and LDA results from Ref. [14], and crosses to experimental values [5,7,9,19]. The dashed lines are only guides to the eye.

Fig. 3: Total and partial electronic density of states (DOS) for Cu-In compounds: a) δ-Cu_7In_3 (aP40), b) $Cu_{11}In_9$ (mC20) and c) $CuIn_2$ (tI12). The site decomposed DOS with their angular momentum, s, p and d band contributions, are plotted. The origin of the energy scale corresponds to the Fermi level.

Fig. 4: Total and partial electronic density of states (DOS) for Cu-Sn compounds: a) -$Cu_{10}Sn_3$ (hP26), b) -Cu_3Sn (oP8) and c) ´-Cu_6Sn_5 (mC44). The site decomposed DOS with their angular momentum, s, p and d band contributions, are plotted. The origin of the energy scale corresponds to the Fermi level.

Fig. 5: Composition dependence of the energy of formation (EOF) from the elements of the Cu-In (a) and Cu-Sn (b) compounds listed in Table 1. Filled symbols correspond to phases stable at low temperature (LT) in the phase diagram; empty symbols to phases stable only at high temperatures (HT). Half-filled symbols represent GGA values for "ideal" B8 parent structures in the Cu-In and Cu-Sn system from Ref. [12] and the present work, respectively.

Fig. 6: The $\Delta(\Delta E^{\phi}(Cu_aM_b)) = \Delta E^{\phi}(Cu_aSn_b) - \Delta E^{\phi}(Cu_aIn_b)$ difference between the energy of formation of various Cu-Sn and Cu-In compounds with the same structure (ϕ) and stoichiometry, according to the present GGA calculations. Filled circles and squares correspond to phases stable at low-temperature (LT) in the Cu-In and Cu-Sn, respectively. Open circles and squares correspond to high temperature (HT) phases of the Cu-In and Cu-Sn systems, respectively. Filled triangles represent the $\Delta(\Delta E^{\phi}(Cu_aM_b))$ differences obtained from the thermodynamic parameters for -$Cu_7(In,Sn)_3$ and -$Cu_3(In,Sn)$ compounds reported in Ref. [13]. For comparisons with the theoretical trends, the $\Delta(\Delta E^{\phi}(Cu_aM_b))$ differences

corresponding to the $Cu_{41}(In,Sn)_{11}$ and $Cu_{77}(In,Sn)_{23}$ compounds are also included using empty triangles. The solid lines are guides to the eye.

Table 1. Description of the binary phases and structures, the sublattice schemes proposed to model their extensions to the Cu-In-Sn system, and the corresponding "end-member" compounds studied in the present work and those according to Ref. [12].

System	Stable or ideal binary phase	Pearson symbol	Ternary phase "two-sublattice" scheme	Stable and hypothetical "end-member" compounds	
Cu-In	-Cu_7In_3 (30 at.% In)	aP40	$Cu_7(In,Sn)_3$	Cu_7In_3	Cu_7Sn_3
	-Cu_9In_4 (30.8 at.% In)	cP52	$Cu_9(In,Sn)_4$	Cu_9In_4	Cu_9Sn_4
	-Cu_2In (33.3 at.% In)	hP6	$Cu_2(In,Sn)_1$	Cu_2In	Cu_2Sn
	$Cu_{10}In_7$ (41 at.% In)	mC68	$Cu_{10}(In,Sn)_7$	$Cu_{10}In_7$	$Cu_{10}Sn_7$
	$Cu_{11}In_9$ (45 at.% In)	mC20	$Cu_{11}(In,Sn)_9$	$Cu_{11}In_9$	$Cu_{11}Sn_9$
	CuIn (50 at.% In)	hP4	$Cu(In,Sn)_1$	CuIn	CuSn
	$CuIn_2$ (66.7 at.%In)	tI12	$Cu_1(In,Sn)_2$	$CuIn_2$	$CuSn_2$
	$CuIn_2$ (66.7 at.%In)	hP6	$Cu_1(In,Sn)_2$	$CuIn_2$	$CuSn_2$
Cu-Sn	-Cu_4Sn (20 at.% Sn)	cF16	$Cu_4(In,Sn)_1$	Cu_4In	Cu_4Sn
	-$Cu_{10}Sn_3$ (23 at.% Sn)	hP26	$Cu_{10}(In,Sn)_3$	$Cu_{10}In_3$	$Cu_{10}Sn_3$
	-Cu_3Sn (25 at.% Sn)	oP8	$Cu_3(In,Sn)_1$	Cu_3In	Cu_3Sn
	-Cu_3Sn (25 at.% Sn)	oP80	$Cu_3(In,Sn)_1$	Cu_3In	Cu_3Sn
	$_1$-Cu_5Sn_4 (44.44 at.% Sn)	mP36	$Cu_5(In,Sn)_4$	Cu_5In_4	Cu_5Sn_4
	$_2$-Cu_5Sn_4 (44.44 at.% Sn)	mC54	$Cu_5(In,Sn)_4$	Cu_5In_4	Cu_5Sn_4
	´-Cu_6Sn_5 (45.45 at.% Sn)	mC44	$Cu_6(In,Sn)_5$	Cu_6In_5	Cu_6Sn_5

Table 2. Calculated structural and equation-of-state parameters for pure elements Cu, In and Sn at 0 K. The lattice parameters are given in Å, the equilibrium volume (V_o) in $Å^3$/atom, the bulk modulus (B_o) in GPa.

Phase	Space group	V_o	a, c, c/a	B_0	B_0´	Aprox.	Ref.
Cu-fcc	Fm3m	12.020	3.636	142.3	3.6	GGA	[12]
		10.948	3.525	182.8	6.3	LDA	Present work
		11.625	3.596[a]	142.0[b]	5.5, 5.0[c]	Exp.	
In-tI2	I4/mmm	27.512	3.305, 5.036, 1.524	36.4	4.7	GGA	[12]
		24.740	3.175, 4.909, 1.546	51.4	5.3	LDA	Present work
		26.020	3.245, 4.942, 1.523[d]	41.8[e]	4.8[e]	Exp.	
Sn-tI4	$I4_1$/amd	28.348	5.947, 3.206, 0.539	48.7	5.0	GGA	Present work
		28.443	5.947, 3.218, 0.541	46.0	4.3	GGA	[14]
		26.883	5.820, 3.175 0.546[d]	57.9[f]	6.01, 4.96[c]	Exp.	

[a] Experimental data extrapolated to 0 K [44,45].

[b] Experimental data at 0 K [46].

[c] Experimental data at 298 K [47].

[d] Experimental data [19].

[e] Experimental data at 293 K [31].

[f] Experimental data at 4.2 K [48].

Table 3 Structural and elastic properties for Cu-In intermetallic phases at 0 K. The lattice parameters are given in Å, the equilibrium volume (V_o) in Å^3/atom, the bulk modulus (B_o) in GPa.

Phase	Space group	V_o	a, b, c , ,	B_0	B_0'	Aprox.	Ref.
Stable							
Cu_7In_3 (aP40)	P-1	15.096	10.183, 9.205, 6.779, 90.17°, 82.92°, 106.62°	99.3	6.0	GGA	Present work
		13.749	9.870, 8.923, 6.569, 90.14°, 82.98°, 106.59°	135.8	5.5	LDA	Present work
		14.695	10.071, 9.126, 6.724, 90.22°, 82.84°, 106.81°			Exp.	[19]
Cu_9In_4 (cP52)	P-43m	15.143	9.234	101.1	5.2	GGA	Present work
		13.798	8.952	137.0	4.7	LDA	Present work
		14.477	9.097			Exp.	[19]
$Cu_{10}In_7$ (mC68)	C2/m	16.841	14.000, 12.047, 6.790, 90.00º	86.2	6.5	GGA	[12]
		15.321	13.570, 11.658, 6.586, 91.02°	118.0	5.6	LDA	Present work
		16.251	13.845, 11.846, 6.739, 91.06º				[7]
$Cu_{11}In_9$ (mC20)	C2/m	17.369	13.027, 4.406, 7.460, 54.22°	81.5	6.7	GGA	[12]
		15.830	12.606, 4.270, 7.230, 54.43º	110.9	4.4	LDA	Present work
		16.697	12.814, 4.354, 7.353, 54.49º				[19]
$CuIn_2$ (tI12)	I4/mcm	20.506	6.723, 5.445	62.6	7.2	GGA	Present work
		18.553	6.503, 5.264	84.4	5.9	LDA	Present work
		19.782	6.645, 5.376				[5]
"Ideal" B8-type (non stable)							
Cu_2In (hP6)	$P6_3/mmc$	15.534	4.471, 5.384	92.1	4.7	GGA	[12]
CuIn (hP4)	$P6_3/mmc$	19.415	4.250, 4.965	76.3	4.8	GGA	[12]
$CuIn_2$ (hP6)	$P6_3/mmc$	22.131	4.606, 7.228	49.9	3.0	GGA	[12]

Table 4 Calculated structural and elastic properties for Cu-Sn intermetallic phases at 0 K. The lattice parameters are given in Å, the equilibrium volume (V_o) in Å^3/atom, the bulk modulus (B_o) in GPa.

Phase	Space group	V_o	a, b, c , ,	B_0	B_0'	Ref.
Stable						
Cu_4Sn (cF16)	F-43m	14.726	6.176	99.6	5.7	Present work
		14.312	6.118			[19]
$Cu_{10}Sn_3$ (hP26)	$P6_3$	14.506	7.386, 7.983	109.4	4.2	Present work
		14.074	7.330, 7.864			[19]
Cu_3Sn (oP8)	Pmmn	14.701	5.559, 4.329, 4.887	104.2	5.5	Present work
		13.590	5.464, 4.256, 4.675	132.2[a]		[18]
		14.052	5.490, 4.320, 4.740			[19]

Cu_3Sn (oP80)	Cmcm	14.683	5.550, 48.835, 4.334	101.8	5.5	Present work
		14.607	5.516, 48.790, 4.342	133.4[a]		[17]
		14.266	5.529, 47.750, 4.323			[19]
Cu_5Sn_4- $_1$ (mP36)	$P2_1/c$	18.220	10.044, 7.403, 9.992 61.99°	81.7	5.4	Present work
		18.282	10.057, 7.416, 10.001 61.89°	81.7	5.0	[14]
		17.309	9.830, 7.270, 9.830 62.5°			[9]
Cu_5Sn_4- $_2$ (mC54)	C2	18.239	12.859, 7.430, 10.309 89.60º	81.1	5.0	Present work
		18.323	12.914, 7.420, 10.325 89.60°	81.5 84.6[b]	5.0	[14]
		17.303	12.600, 7.270, 10.200 90°			[9]
Cu_6Sn_5- (mC44)	C2/c	18.428	11.134, 7.375, 9.989 98.71°	80.9	5.1	Present work
		18.512	11.138, 7.403, 9.995 98.65°	79.6 84.4[b]	5.0	[14]
		17.777	11.036, 7.288, 9.841 98.81°			[9]
"Ideal" B8-type (non stable)						
Cu_2Sn (hP6)	$P6_3/mmc$	16.366	4.516 , 5.558	87.9	5.3	Present work
		16.352	4.523, 5.543	88.0	4.9	[14]
CuSn (hP4)	$P6_3/mmc$	19.335	4.189, 5.090	75.1	4.6	Present work
		19.350	4.190, 5.092	76.5	5.1	[14]
$CuSn_2$ (hP6)	$P6_3/mmc$	23.413	4.482, 8.076	50.2	3.4	Present work
		23.406	4.479, 8.089	49.4	4.9	[14]

[a] Polycrystalline bulk modulus obtained from the *ab initio* calculated single crystal elastic constants using the Voigt method.

[b] Experimental data at 298 K [14].

Table 5 Unit cell internal coordinates of Cu_7In_3, Cu_9In_4 and $CuIn_2$ obtained from our *ab initio* calculations and experimental data from Ref. [19].

Phase	Space group	Internal Coordinates (x, y, z)			
		Atom	Wyck.	Present calculation	Experimental
Cu-In					
Cu_7In_3	P-1	Cu1	1a	0.0000, 0.0000, 0.0000	0.000, 0.000, 0.000
		Cu2	1d	0.5000, 0.0000, 0.0000	0.500, 0.000, 0.000
		Cu3	2i	0.0636, 0.8532, 0.3014	0.061, 0.855, 0.304
		Cu4	2i	0.6961, 0.5406, 0.8452	0.696, 0.541, 0.843
		Cu5	2i	0.7725, 0.4269, 0.1536	0.772, 0.428, 0.153
		Cu6	2i	0.8662, 0.2933, 0.4394	0.866, 0.294, 0.444
		Cu7	2i	0.5864, 0.8503, 0.2739	0.582, 0.850, 0.273
		Cu8	2i	0.8394, 0.9968, 0.3351	0.838, 0.998, 0.339
		Cu9	2i	0.6640, 0.1423, 0.2428	0.664, 0.143, 0.245
		Cu10	2i	0.6514, 0.6901, 0.5427	0.654, 0.694, 0.539
		Cu11	2i	0.7136, 0.2393, 0.8595	0.713, 0.240, 0.856
		Cu12	2i	0.2496, 0.0172, 0.0310	0.251, 0.019, 0.033
		Cu13	2i	0.4350, 0.4500, 0.7722	0.437, 0.450, 0.773

		Cu14	2i	0.8647, 0.5876, 0.4717	0.866, 0.587, 0.471
		Cu15	2i	0.9140, 0.2345, 0.0695	0.915, 0.235, 0.069
		In1	2i	0.9428, 0.4716, 0.7909	0.944, 0.472, 0.793
		In2	2i	0.6350, 0.0068, 0.6186	0.634, 0.006, 0.618
		In3	2i	0.5173, 0.7184, 0.9237	0.518, 0.720, 0.921
		In4	2i	0.8183, 0.7351, 0.1427	0.817, 0.735, 0.142
		In5	2i	0.1050, 0.1614, 0.3272	0.104, 0.164, 0.322
		In6	2i	0.6214, 0.3624, 0.5213	0.621, 0.364, 0.518
Cu_9In_4	P-43m	Cu1	4e	0.3313, 0.3313, 0.3313	0.3248, 0.3248, 0.3248
		Cu2	4e	0.5979, 0.5979, 0.5979	0.6052, 0.6052, 0.6052
		Cu3	4e	0.8343, 0.8343, 0.8343	0.8035, 0.8053, 0.8053
		Cu4	6f	0.3580, 0.0000, 0.0000	0.3561, 0.0000, 0.0000
		Cu5	6g	0.8533, 0.5000, 0.5000	0.8559, 0.5000, 0.5000
		Cu6	12i	0.3254, 0.3254, 0.0283	0.3145, 0.3145, 0.0329
		In1	4e	0.1329, 0.1329, 0.1329	0.1151, 0.1151, 0.1151
		In2	12i	0.8085, 0.8085, 0.5353	0.8089, 0.8089, 0.5360
$CuIn_2$	I4/mcm	Cu	4a	0.0000, 0.0000, 0.5000	
		In	8h	0.1627, 0.6627, 0.0000	

Table 6 Unit cell internal coordinates of $Cu_{10}Sn_3$, Cu_3Sn, Cu_5Sn_4-$_1$, Cu_5Sn_4-$_2$ and Cu_6Sn_5-′ obtained from our *ab initio* calculations and experimental data [9,19].

Phase	Space group	Internal Coordinates (x, y, z)			
		Atom	Wyck.	Present calculation	Experimental
Cu-Sn					
$Cu_{10}Sn_3$	$P6_3$	Cu1	2a	0.0000, 0.0000, 0.9944	0.0000, 0.0000, 0.9777[a]
		Cu2	2b	0.3333, 0.6667, 0.4197	0.3333, 0.6667, 0.4100
		Cu3	2b	0.3333, 0.6667, 0.0736	0.3333, 0.6667, 0.0737
		Cu4	2b	0.3333, 0.6667, 0.7465	0.3333, 0.6667, 0.7450
		Cu5	6c	0.6413, 0.9712, 0.9129	0.6472, 0.9821, 0.9155
		Cu6	6c	0.3583, 0.0287, 0.0800	0.3574, 0.0350, 0.0831
		Sn	6c	0.6844, 0.9768, 0.2500	0.6800, 0.9800, 0.2500
Cu_3Sn	Pmmn	Cu1	2b	0.0000, 0.5000, 0.7050	0.0000, 0.5000, 0.6670[a]
		Cu2	4f	0.2500, 0.0000, 0.8460	0.2500, 0.0000, 0.8330
		Sn	2a	0.0000, 0,0000, 0.3449	0.0000, 0.0000, 0.3330
Cu_3Sn	Cmcm	Cu1	4c	0.0000, 0.0698, 0.2500	0.0000, 0.0682, 0.2500[a]
		Cu2	4c	0.0000, 0.1705, 0.2500	0.0000, 0.1690, 0.2500
		Cu3	4c	0.0000, 0.2707, 0.2500	0.0000, 0.2690, 0.2500
		Cu4	4c	0.0000, 0.3710, 0.2500	0.0000, 0.3693, 0.2500
		Cu5	4c	0.0000, 0.4699, 0.2500	0.0000, 0.4688, 0.2500
		Cu6	8g	0.2628, 0.0155, 0.2500	0.2607, 0.0158, 0.2500
		Cu7	8g	0.2517, 0.1153, 0.2500	0.2514, 0.1157, 0.2500
		Cu8	8g	0.2537, 0.2153, 0.2500	0.2508, 0.2159, 0.2500
		Cu9	8g	0.2542, 0.3154, 0.2500	0.2525, 0.3159, 0.2500
		Cu10	8g	0.2566, 0.4156, 0.2500	0.2528, 0.4159, 0.2500
		Sn1	4c	0.0000, 0.9659, 0.2500	0.0000, 0.9663, 0.2500
		Sn2	4c	0.0000, 0.8653, 0.2500	0.0000, 0.8661, 0.2500
		Sn3	4c	0.0000, 0.7653, 0.2500	0.0000, 0.7662, 0.2500
		Sn4	4c	0.0000, 0.6654, 0.2500	0.0000, 0.6663, 0.2500
		Sn5	4c	0.0000, 0.5661, 0.2500	0.0000, 0.5666, 0.2500
Cu_5Sn_4-$_1$	$P2_1/c$	Cu1	4e	0.0560, 0.7749, 0.0575	0.057, 0.779, 0.056[b]
		Cu2	4e	0.1895, 0.2559, 0.1867	0.189, 0.253, 0.187
		Cu3	4e	0.1916, 0.0874, 0.9378	0.188, 0.090, 0.937
		Cu4	4e	0.3161, 0.7256, 0.3178	0.317, 0.725, 0.321

		Cu5	4e	0.4298, 0.2434, 0.4315	0.427, 0.258, 0.427
		Sn1	4e	0.0711, 0.5986, 0.2853	0.071, 0.597, 0.287
		Sn2	4e	0.1833, 0.0534, 0.4356	0.180, 0.057, 0.440
		Sn3	4e	0.3245, 0.5848, 0.5779	0.313, 0.590, 0.583
		Sn4	4e	0.4561, 0.0941, 0.6686	0.451, 0.087, 0.663
Cu_5Sn_4- 2	C2	Cu1	2a	0.0000, 0.6785, 0.0000	0.000, 0.691, 0.000[b]
		Cu2	4c	0.0084, 0.0122, 0.3767	0.015, 0.030, 0.374
		Cu3	4c	0.0076, 0.9962, 0.1256	0.022, 0.007, 0.127
		Cu4	4c	0.1710, 0.8567, 0.2505	0.173, 0.853, 0.254
		Cu5	4c	0.3263, 0.0131, 0.3771	0.326, 0.000, 0.379
		Cu6	4c	0.3339, 0.0200, 0.1257	0.343, 0.017, 0.129
		Cu7	4c	0.6607, 0.0414, 0.1256	0.653, 0.034, 0.133
		Cu8	4c	0.6686, 0.0361, 0.3765	0.666, 0.036, 0.379
		Sn1	2a	0.0000, 0.3217, 0.0000	0.000, 0.333, 0.000
		Sn2	2b	0.0000, 0.3481, 0.5000	0.000, 0.360, 0.500
		Sn3	4c	0.1635, 0.2141, 0.2496	0.179, 0.210, 0.249
		Sn4	4c	0.3210, 0.3651, 0.0188	0.307, 0.349, 0.009
		Sn5	4c	0.3312, 0.3559, 0.4806	0.339, 0.352, 0.477
		Sn6	4c	0.4911, 0.1700, 0.2686	0.488, 0.190, 0.268
		Sn7	4c	0.8503, 0.1789, 0.2495	0.845, 0.164, 0.240
Cu_6Sn_5- ´	C2/c	Cu1	4a	0.0000, 0.0000, 0.0000	0.000, 0.000, 0.000[b]
		Cu2	4e	0.0000, 0.1610, 0.2500	0.000, 0.160, 0.250
		Cu3	8f	0.1015, 0.4731, 0.2036	0.101, 0.473, 0.202
		Cu4	8f	0.3068, 0.5052, 0.6092	0.306, 0.504, 0.610
		Sn1	4e	0.0000, 0.7998, 0.2500	0.000, 0.799, 0.250
		Sn2	8f	0.2865, 0.6546, 0.3573	0.285, 0.655, 0.358
		Sn3	8f	0.3917, 0.1624, 0.5288	0.391, 0.162, 0.529

[a] Ref. [19].

[b] Ref. [9].

Table 7. Average number of Cu-Cu nearest neighbours (NN) and nearest neighbor distances (NND) (in Å) (Cu-Cu, Cu-X, and X-X; X = In, Sn) for selected Cu-In and Cu-Sn compounds.

	Space group	**NN (Cu-Cu)**	**NND(Cu-Cu)**	**NND(Cu-X)**	**NND(X-X)**
Cu-In					
Cu_7In_3	P-1	7.14	2.68	2.82	3.56
$Cu_{11}In_9$	C2/m	4.91	2.75	2.80	3.16
$CuIn_2$	I4/mcm	2	2.72	2.86	3.42
Cu-Sn					
$Cu_{10}Sn_3$	$P6_3$	7.8	2.67	2.82	
Cu_3Sn	Pmmn	8	2.73	2.78	
Cu_6Sn_5- ´	C2/c	3.2	2.65	2.78	3.38

Table 8 Energy of formation (in kJ/mol-atom) for Cu-In intermetallic phases at 0 K obtained by *ab initio* calculations, CALPHAD modeling and experiments. Reference states are Cu-fcc and In-tI2.

Phase	Space group	Energy of Formation			
		Ab initio calculations		CALPHAD-type Thermodynamic calculation	Experimental
Stable					
Cu_7In_3	P-1	-1.179	GGA	-7.991 [a]	-8.620 [b]
		-3.758	LDA		
Cu_9In_4	P-43m	0.271	GGA	-5.542 [c]	-3.874 [d]
		-2.283	LDA		
$Cu_{10}In_7$	C2/m	-1.744 [e]	GGA		
		-4.648	LDA		
$Cu_{11}In_9$	C2/m	-0.825 [e]	GGA	-7.526 [a]	
		-3.881	LDA		
$CuIn_2$	I4/mcm	-0.240	GGA		
		-2.701	LDA		
"Ideal" B8-type (non stable)					
Cu_2In	$P6_3/mmc$	7.631 [e]	GGA		
CuIn	$P6_3/mmc$	2.420 [e]	GGA		
$CuIn_2$	$P6_3/mmc$	15.150 [e]	GGA		
Hypothetical					
Cu_4In	F-43m	3.835	GGA		
$Cu_{10}In_3$	$P6_3$	0.353	GGA		
Cu_3In	Pmmn	0.803	GGA		
Cu_3In	Cmcm	1.004	GGA		
Cu_5In_4-$_1$	$P2_1/c$	-1.073	GGA		
Cu_5In_4-$_2$	C2	-0.921	GGA		
Cu_6In_5-	C2/c	-0.778	GGA		

[a] Enthalpy of formation at 298 K from Liu *et al.* [49].

[b] Enthalpy of formation at T = 298 K from Dichi *et al.* [50].

[c] Enthalpy of formation at T = 941 K and 30.87 at% In from Liu *et al.* [49].

[d] Enthalpy of formation at T = 941 K and 30.87 at% In from Kang *et al.* [51].

[e] *Ab initio* calculated values from Ramos de Debiaggi *et al.* [12].

Table 9 Energy of formation (in kJ/mol-atom) for Cu-Sn intermetallic phases at 0 K obtained by *ab initio* calculations, CALPHAD modeling and experiments. Reference states are Cu-fcc and Sn-tI4.

Phase	Space group	Energy of Formation			
		Ab initio calculations		CALPHAD-type Thermodynamic calculation	Experimental
Stable					
Cu_4Sn	F-43m	5.796	GGA		
$Cu_{10}Sn_3$	$P6_3$	0.664	GGA	-6.655 [a]	
Cu_3Sn	Pmmn	-0.072	GGA	-8.194 [a]	-7.824 [b]
Cu_3Sn	Cmcm	0.073	GGA		
Cu_5Sn_4-$_1$	$P2_1/c$	-2.962	GGA		
		-2.884 [c]	GGA		
		-3.666 [c]	LDA		
Cu_5Sn_4-$_2$	C2	-2.611	GGA	-6.870 [a]	
		-2.595 [c]	GGA	-7.086 [d]	
		-3.271 [c]	LDA	7.444 [e]	

Cu_6Sn_5-´	C2/c	-3.351	GGA	-7.130 [a]	-7.037 [f]
		-3.205 [c]	GGA	-7.346 [d]	
		-4.020 [c]	LDA	-7.748 [e]	
"Ideal" B8-type (non stable)					
Cu_2Sn	$P6_3/mmc$	13.960	GGA		
		14.472 [c]	GGA		
		16.752 [c]	LDA		
CuSn	$P6_3/mmc$	-4.715	GGA		
		-4.485 [c]	GGA		
		-5.458 [c]	LDA		
$CuSn_2$	$P6_3/mmc$	15.016	GGA		
		15.455 [c]	GGA		
		19.804 [c]	LDA		
Hypothetical					
Cu_7Sn_3	P-1	2.426	GGA		
Cu_9Sn_4	P-43m	5.712	GGA		
$Cu_{10}Sn_7$	C2/m	3.853	GGA		
$Cu_{11}Sn_9$	C2/m	5.288	GGA		
$CuSn_2$	I4/mcm	1.895	GGA		

[a] Shim *et al.* [52].

[b] Experimental data at T = 293 K [53].

[c] Calculated US-PP values by Ghosh *et al.* [14].

[d] Moon *et al.* [54].

[e] Liu *et al.* [55].

[f] Gangulee *et al.* [42].

Research highlights

A DFT study of Cu-In and Cu-Sn compounds in Cu-In-Sn soldering alloys is reported
Structural, cohesive, electronic and thermodynamic trends are established
Phase-stabilities at low T are well reproduced by the 0K thermodynamic values
Available structural and equation-of-state data are satisfactorily accounted for
Experimental and CALPHAD-based relative-stability properties are well reproduced

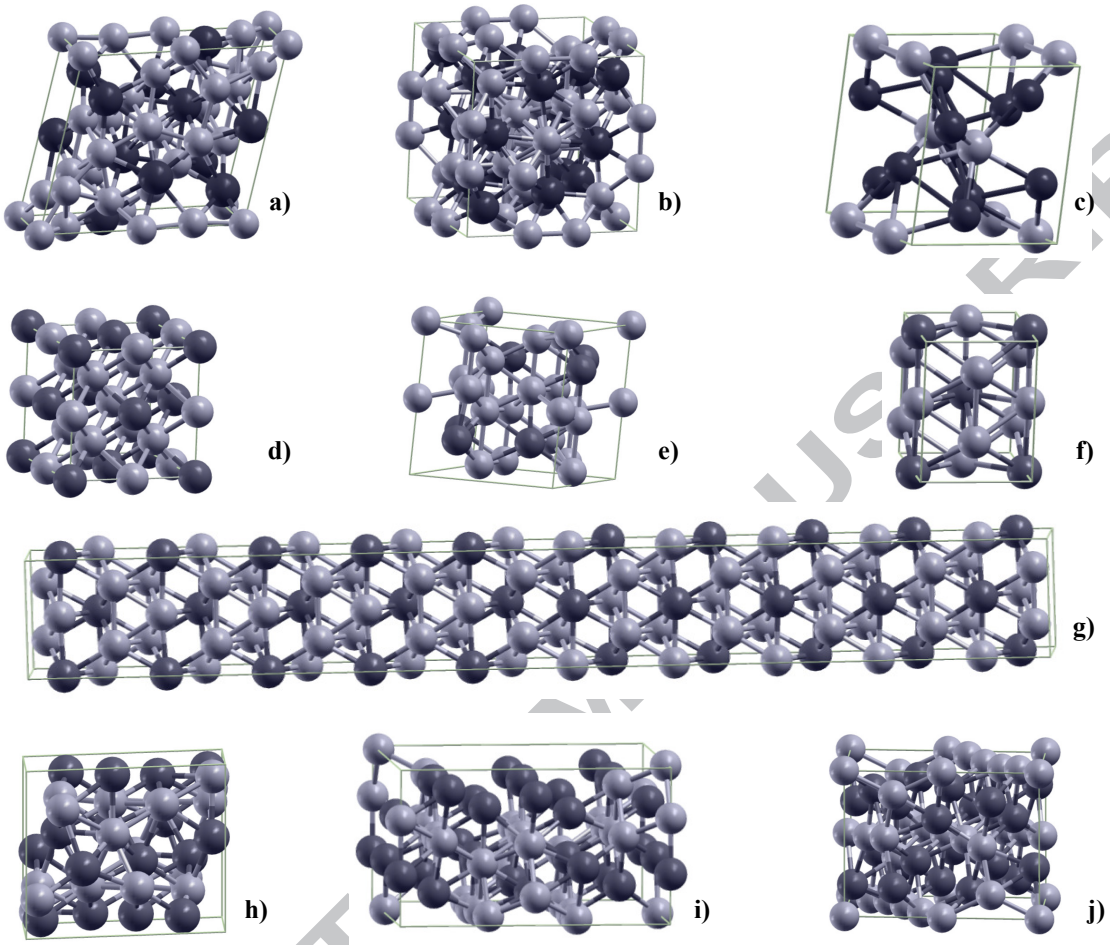

Fig. 1

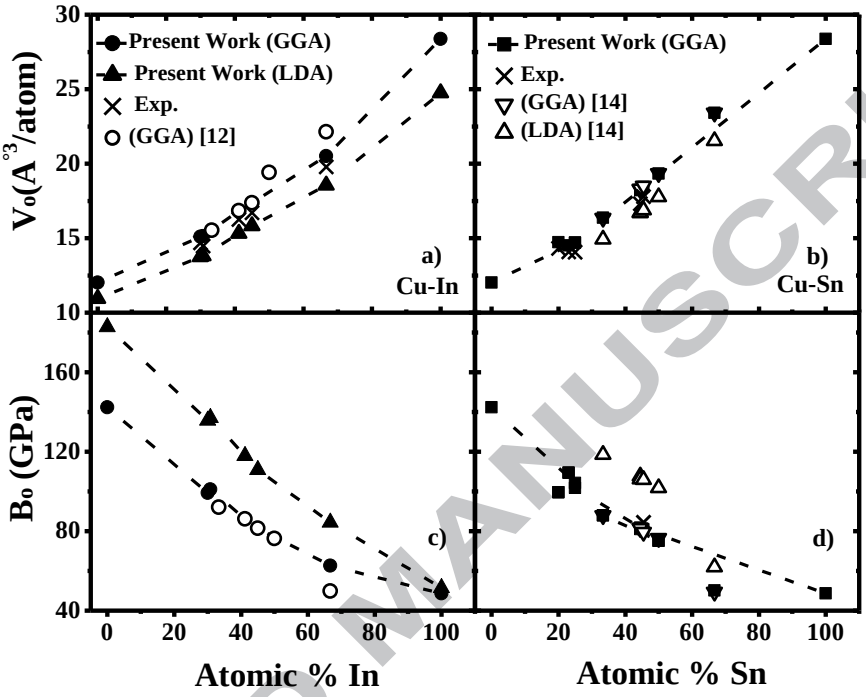

Fig. 2

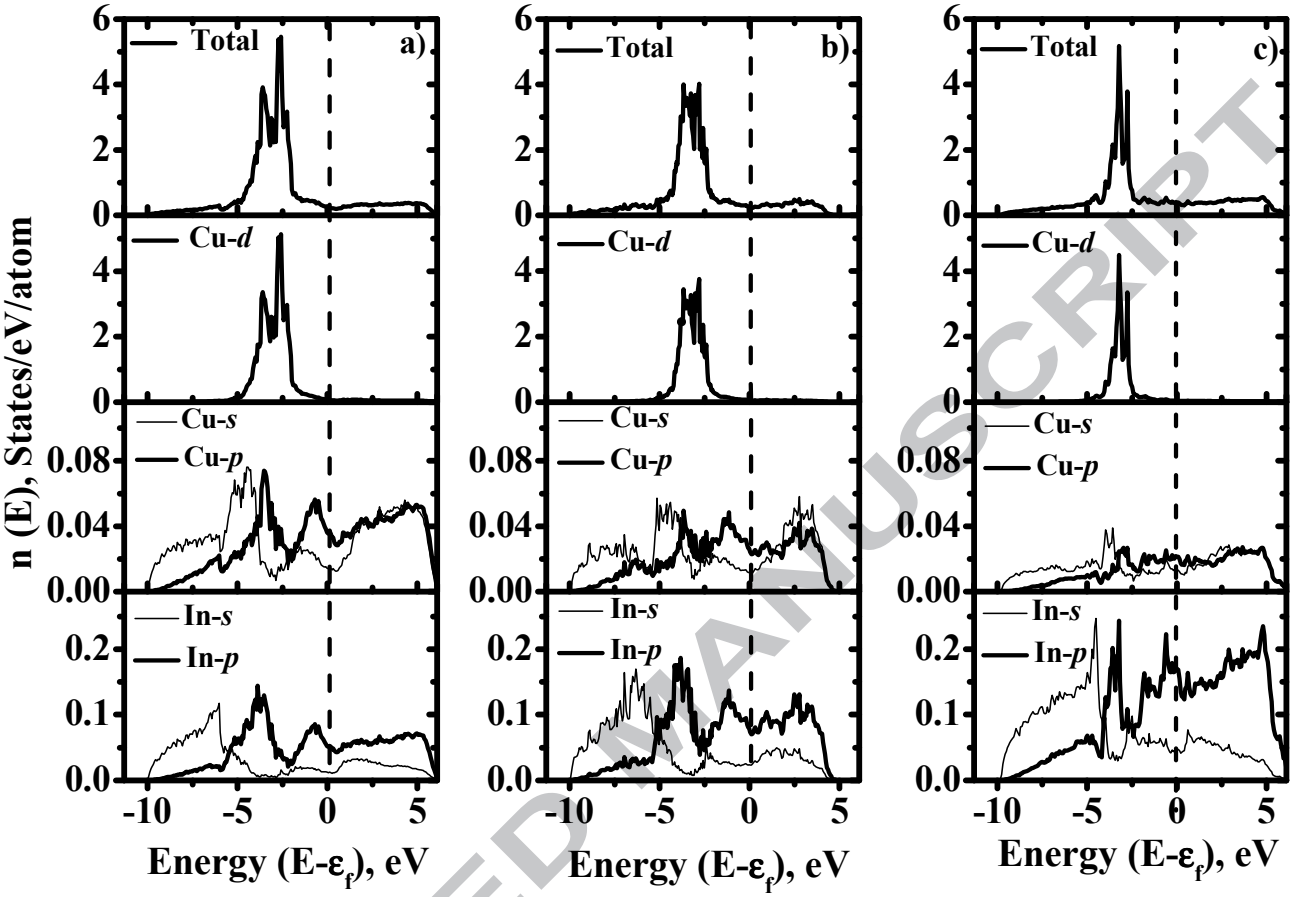

Fig. 3

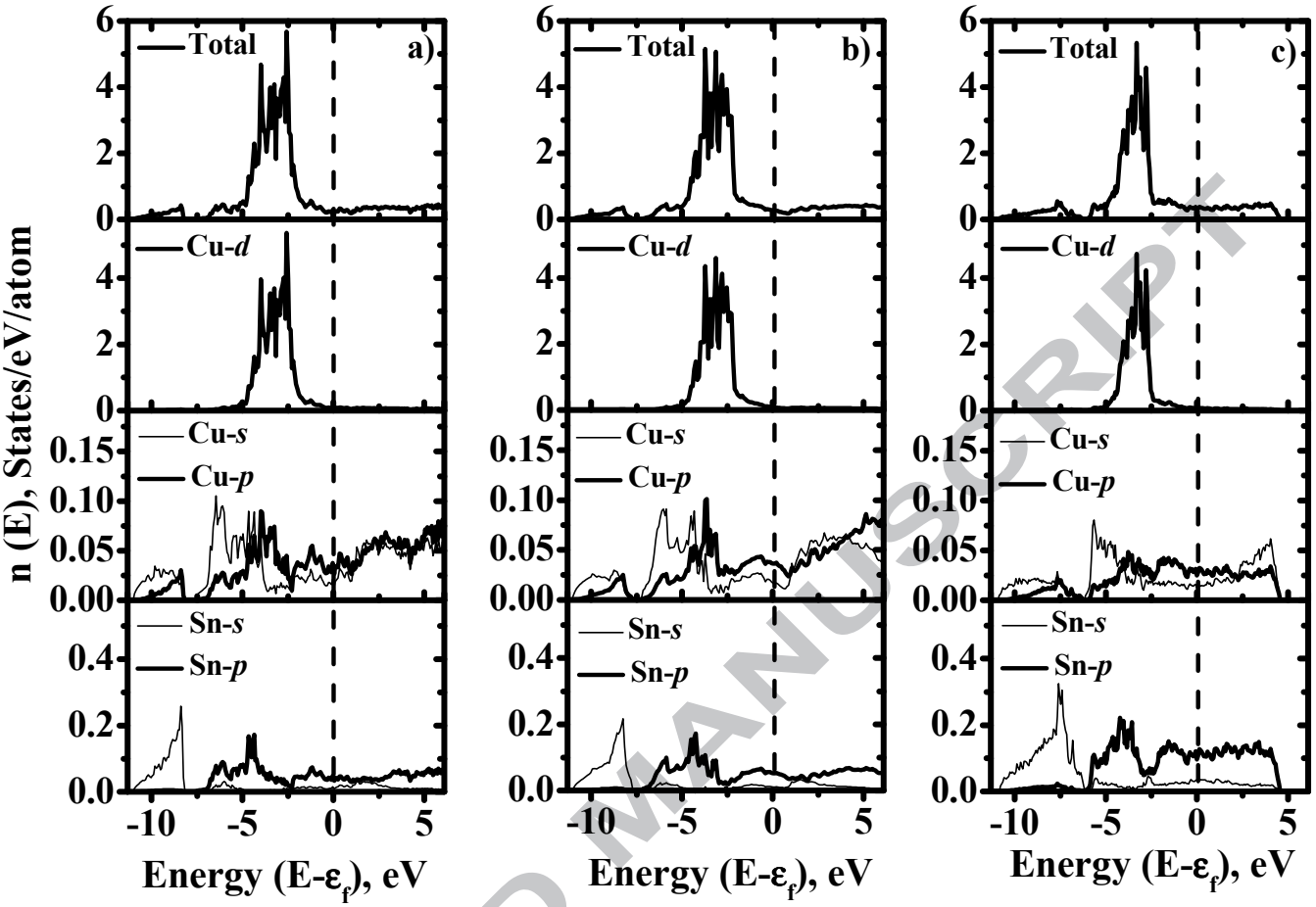

Fig. 4

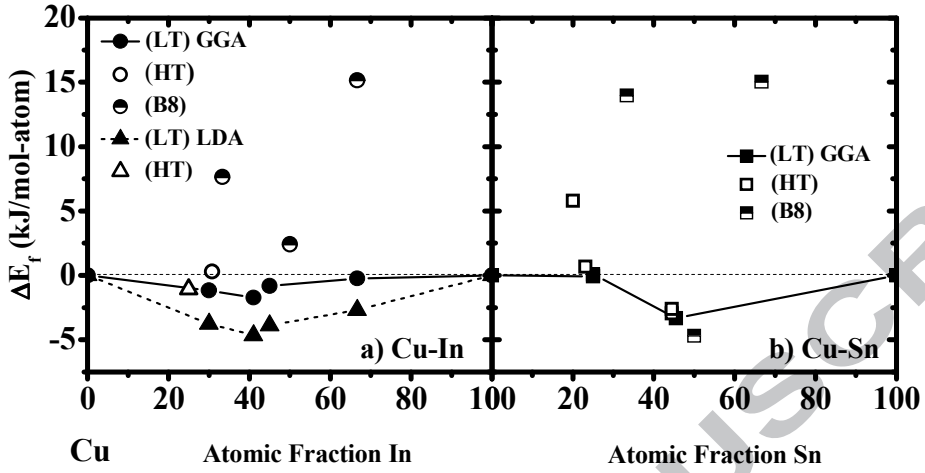

Fig. 5

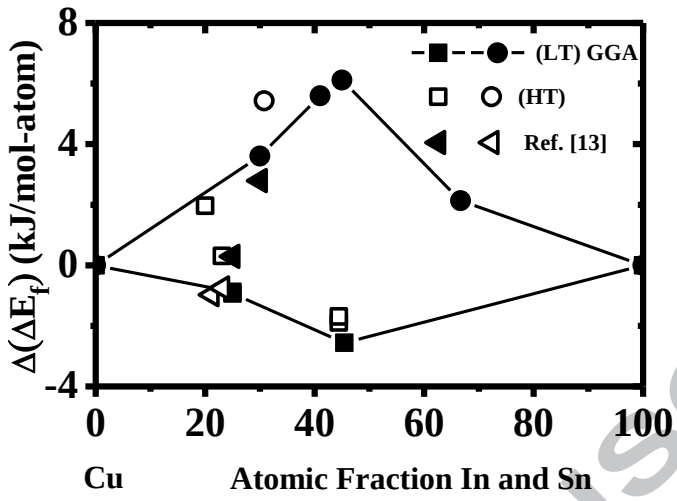

Fig. 6